Multidimensional GC–Fourier Transform Ion Cyclotron Resonance MS Analyses: Utilizing Gas-Phase Basicities to Characterize Multicomponent Gasoline Samples

Zhaohui Luo, Caleb Heffner, and **Touradj Solouki***
Department of Chemistry, University of Maine, Orono, ME 04469

Abstract

Hydrocarbon isomers, present in crude petroleum, may yield similar gas chromatography (GC) retention times and indistinguishable mass spectral patterns. Hence, conventional GC–mass spectrometry (MS) may not provide sufficient data for identification of hydrocarbon isomers. Real-time proton affinity or gas-phase basicity "bracketing" provides an additional dimension to GC–MS analyses. Our GC–fourier transform (FT)-ion cyclotron resonance (ICR)-MS yielded an average mass measurement error of less than 3 ppm for components of a retail gasoline sample. The combined use of concurrent thermo-chemical measurements with GC–FT-ICR-MS data analysis allowed differentiation of various isomers such as C_8H_{10} species.

Introduction

Historically, the need for characterization of complex hydrocarbon systems has contributed to enormous technological advances and integration of analytical approaches (1–3). For example, crude oil is a complex mixture of several thousand compounds and the need for its complete characterization is the driving force behind the emerging field of petroleomics (4). Components present in a petroleum mixture include hydrocarbons (from simple alkanes to complex aliphatic components) and a number of low concentration polar compounds (such as thiophenoaromatics and sulfides and NSO-containing compounds) (5,6). The composition of crude oil from different sources can be different and hence complete characterization of these samples can lead to source identification; such endeavors are often desirable in forensic and environmental sciences. For instance, even refined gasoline products of different brands can be slightly different from each other and thus "fingerprinting" crude oil or refined petroleum products is very important for suspected arson case investigations (7–11). Advances in analytical methodologies also play significant roles in identifying environmental contaminants in air, water, and soil as well as developing remediation processes (12) and regulatory procedures (13).

A significant amount of research has been devoted to fingerprinting crude oil and petroleum products for the protection of the environment and forensic criminal investigations (4,6,11,14–16). Techniques such as gas chromatography–flame ionization detector (GC–FID) and two dimensional GC×GC are widely used for characterizing components in oil samples from different locations or sources. Interpretation of the results from these methods relies on comparisons and contrasts between retention time tables for standard chemicals. GC retention times depend on various experimental parameters such as GC temperature or pressure programming, GC column type, and head pressure; changing these experimental variables often yields test specific results. Therefore, it is not suitable to use retention times (or retention indices) alone to identify unknown molecules or confirm their identity at a high level of confidence.

The use of additional molecular characteristics such as PAs or GBs can improve the success rate for unknown analyses. Often, environmental samples require high analytical sensitivity and preclude the use of conventional and powerful analytical techniques such as nuclear magnetic resonance (17,18). However, modern mass spectrometry techniques such as time of flight (19), LC–ESI-FT-ion cyclotron resonance ICR (20), and GC–FT-ICR (8,21) offer high sensitivity. Although conventional two-dimensional GC experiments are quite useful to handle complex mixtures and separate various components, data can not be used to establish unknown identities. For example, GC retention times can vary depending on the experimental parameters employed. However, true values of thermochemical properties, such as the proton affinity, are independent of the experimental procedures employed and can provide invaluable data for unknown determinations. Ion-molecule reactions offer an excellent opportunity to measure thermochemical data such as PAs. For instance, PAs of GC eluted compounds can be determined in FT-ICR experiments and these experimental values can be compared with the available data (22) or theoretically predicted values for highly competent unknown identification. Therefore, in addition to the mass measurement accuracy, FT-ICR offers supplementary multidimensional advantages such as thermochemical measurements by ion-molecule reactions.

The combination of GC (for analyte separation) with MS (as the detector) is a powerful tool that has been applied to various scientific fields and is an integral part of environmental analysis (14,23–25). The use of a mass spectrometer as a detector is

* Author to whom correspondence should be addressed.

attractive because it can provide molecular weight and structural information (e.g., mass spectral fragmentation patterns). A conventional EI-GC–MS experiment yields information about the analytes' retention times (RT) and *m/z* values; however, this information alone (i.e., RT and mass spectral data) may not be sufficient to assign identities of unknown molecules. For example, the fragmentation pattern and mass spectral database libraries that are used for unknown identification may not exist for a true "unknown" (24), and therefore other types of information are needed for reliable molecular identification. In this respect, FT-ICR-MS offers unique advantages such as high mass measurement accuracy (MMA < 5 ppm), high mass resolving power (MRP or m/Δm 50% > 100,000), and an ability to carry out ion-molecule reactions that improve analytical resolution for molecular identification. Although achievable MMA with FT-ICR-MS is sufficient to determine elemental compositions (8,26–28), it is an analytical challenge to distinguish isomers by using GC mass spectral data alone. Often molecular isomers co-elute from the GC column, and their mass spectral pattern can be indistinguishable. Several studies have focused on employing ion-molecule reactions to analyze complex mixtures such as gasoline (29–31). For example, gas phase ion-molecule reactions can aid to locate double bond positions in alkenes (29,30,32,33). Furthermore, Roussis and Fedora employed acetone and acetone-d_6 as chemical ionization (CI) reagents to differentiate isomers of alkenes and cycloalkanes in complex petroleum samples (31). It is our desire to utilize the unique advantages of the FT-ICR-MS and introduce additional analyses dimensions to conventional GC–MS. Here, we demonstrate that the acquisition of thermochemical data (e.g., real-time determination of PAs or GBs) can provide additional information to confirm unknown identities at a higher level of confidence.

Ion-molecule reactions can be monitored in real time, by using selected ion chromatography (SIC) techniques and analyzing the various SICs for different precursor (reactant CI reagent ion) and product ions. In 1966, Munson and Field introduced chemical ionization as a new analytical technique (34,35). Unlike ionization with highly energetic electrons, chemical ionization is a "soft ionization" technique and yields mass spectra with less ion fragmentation (34–37). In our laboratory, a multi-dimensional GC–FT-ICR-MS method was developed and its utility was demonstrated using a mixture of ketone and aromatic compounds (38). Here we demonstrate that proton transfer reactions from protonated reagent ions (e.g., from the self-chemical ionization of ethanol, methanol, isopropanol, acetone, and others) to analyte gasoline molecules can be monitored to provide an additional analytical dimension for sample characterization. The use of chemical ionization (CI) GC–FT-ICR-MS, as demonstrated here, can be used to identify the presence of co-eluting isomers.

Experimental

Chemicals and sample preparation

Ethanol (ACS/UPS grade 200 proof) was purchased from Pharmco (Brookfield, CT). Toluene (Certified ACS), acetone (Certified ACS), 2-propanol (Certified ACS), and methanol (HPLC grade) were purchased from Fisher Scientific (Fair Lawn, NJ). 3-Pentanone (98%), *o*-xylene (98%, HPLC grade), *p*-xylene (99+%, HPLC grade), *m*-xylene (99%), and ethylbenzene (99.8%) were purchased from Sigma-Aldrich Chemical Company (Milwaukee, WI). A 250-mL reservoir connected to a pulsed valve containing CI reagents at pressures of ≤ 1 torr was used for chemical ionization experiments. Conventional freeze-pump-thaw cycles were used to degas the reagents prior to admittance to the evacuated 250-mL reservoir. All of the standard chemicals were used without further purification. Regular (87 Research Octane Number) gasoline samples were collected from various retail gas stations in Orono, Maine (in January). Gasoline samples from four different gas stations were collected, and their GC mass spectral "sample-prints" looked similar but distinguishable; in this paper, we present the multiple ion monitoring GC–FT-ICR-MS results from one of these representative samples. Liquid gasoline sample (10 µL) was transferred into a N_2 filled 40 mL EPA vial using a 25 µL syringe. A 10 µL portion of the head space was withdrawn from the 40 mL vial and injected onto the GC column; analytes were post-GC cryofocused before mass spectral analysis.

Instrumentation

An in-house designed 7 T GC–FT-ICR MS equipped with an SRI model 8610C GC system (SRI Instruments, Las Vegas, NV) and a MTX-1 capillary column (Restek Corporation, Bellefonte, PA) was used for our studies. Design and configuration details of this instrument are published elsewhere (38).

An in-house designed cryofocuser/cold trap was installed between the GC and FT-ICR-MS to improve sensitivity and MRP. The design was based on the work of Jacoby and co-workers (39). It consisted of a capacitive discharge heating unit (powered by a regulated power supply, model LA 50-03BM-0317, Lambda Electronic Corp., NY) controlled by a Dell computer, liquid N_2 container (a ~ 200-mL Teflon cup), and a cryofocusing element (a piece of ~10 cm long and 0.78 mm o.d. Restek GC guard column) where the GC effluent was alternatively cooled/heated. The boiling point of liquid N_2 is ~77 K (22) thus organic compounds eluting from the GC were cooled and solidified in the cryofocuser. The boiling point of helium gas is ~ 4 K (22); therefore, helium carrier gas remained in the gas phase and was pumped away to the exhaust system through the rotary pump. The "frozen" organic molecules were flash heated and pulsed into the ICR cell. A 3-way pulsed valve was used to redirect and switch the cryofocuser outlet either to the exhaust or ICR cell for internal ionization.

GC programming/data analysis

The GC oven temperature was initialized at 60°C for 2 min, ramped at 3°C/min to 180°C, and kept at 180°C until the experiment was terminated.

All of the mass spectral data (including GC–FT-ICR MS or other EI and/or CI mass spectra) were acquired at a 16 MHz analog-to digital converter rate. Generally between 128 k to 512 k data points were acquired for MS analyses. Blackman Harris apodization [without any zero fill(s)] was used for all of the data analyses and mass spectra shown here. Although zero filling can enhance peak shapes to better define peak centroids and improve mass measurement accuracy, here, we report our data under no zero filling conditions to reduce computation time required for true online GC–FT-ICR-MS data analysis.

Ionization methods

CI was utilized for the majority of this study. Electron impact ionization was used in the confirmatory analysis of C_7H_8 standards (see the "Analysis of standard toluene and 1,3,5-cycloheptatriene samples" section) and some gasoline samples. CI reagents were stored in a 250-mL reservoir connected to a pulsed-valve ~1 m away from the ICR cell (38). The pressure inside the reagent reservoir was maintained at ≤ 1 Torr. All CI reagents were introduced into the ICR cell *via* a pulsed valve using operator defined event sequences similar to previously published work (38,40).

Results and Discussion

CI reagents

Figure 1 shows a representative mass spectrum of the CI reagent baseline. The peak at 100% relative abundance corresponds to the protonated ethanol (*m/z* 47). The other species include $C_2H_3O^+$ (*m/z* 43), $C_2H_5O^+$ (*m/z* 45), and $C_4H_{11}O^+$ (*m/z* 75): protonated ketene (41), protonated acetaldehyde (42), and protonated ether (43), respectively. These ions were either ethanol EI fragment ions (e.g., *m/z* 43 and *m/z* 45) or products of self-chemical ionization (SCI) (e.g., *m/z* 47 and *m/z* 75) formed during the reaction delay period (44). Collisions with the He carrier gas atoms assured thermalization of the CI reagent ions and the ion-molecule reaction products (38). Although He is not an efficient collisional cooling gas, under our experimental conditions, CI reagent ions experience thousands of cooling collisions with He atoms pulsed into the ICR cell and become thermalized (38). Moreover, fragment ions corresponding to potential high energy processes were not observed in these experiments. In this experiment, selected reagent ions were used as reference Brönsted acids for proton affinity bracketing. The total ion chromatogram (TIC) for a commercial gasoline sample and sum of all SICs for CI reagents from ethanol SCI reactions are shown in Figure 2. The corresponding individual chromatograms of the CI reagents from the CI GC–FT-ICR-MS analysis of this gasoline sample are shown as SICs in Figure 3. The proton affinities of the conjugate bases (PACB) of the reagent ions are listed above the corresponding SICs for all three reagent ions.

Mass spectral data were acquired 3 min after the sample injection. As it has been discussed in the introduction, when the analyte molecule has a higher PA than the conjugate base of the CI reagent, the analyte molecule can be protonated, yielding a protonated analyte ion, $[A+H]^+$. As a result of the proton transfer, intensity of certain CI reagent ions' SIC will decrease. It should be noted that for the presented PT reactions, we neglected the entropy contributions. For example, entropy differences between the protonated and parent neutral species for aromatic systems can be significant (38). In those cases, variable temperature experiments can yield more reliable PA values. For example, the entropy change for a proton transfer reaction between oxygen bases (e.g., ethers, ketones) is generally small, ≤ 2 cal/mol/K (45). However, for proton transfer reactions between an oxygen base and an aromatic base couple, the half reaction entropy change can be large [e.g., for the couple dimethylether/xylene (*m*, *o*, or *p*), ΔS ranges from ~3 to ~8 cal/mol/K (46)]. Therefore, the TΔS term in ΔG can no longer negligible (1.1–2.9 kcal/mol) under our experimental ICR cell temperature of 360 K. The expression, ΔPA ≈ ΔG can be a poor approximation to use when estimating the proton affinity differences between oxygen base/aromatic base couples. For the present work, qualitative comparisons were sufficient to establish PA bracketing ladders. If the conjugate base of the CI reagent ion has higher PA value (e.g., 4 kcal/mol or more) than the analyte molecule M, no significant proton transfer to the analyte will occur. Therefore, the intensity of CI reagent ions' SIC will be undepleted. Thus, selected ion chromatograms of reagents (e.g., Figure 3) can be used to bracket the PAs of eluting analytes. Previously, we used reactant ion monitoring to determine PA values of GC eluting ketone and aromatic standards (38). Here, we demonstrate the utility of a similar approach for characterizing petroleum refined products and authentic standards.

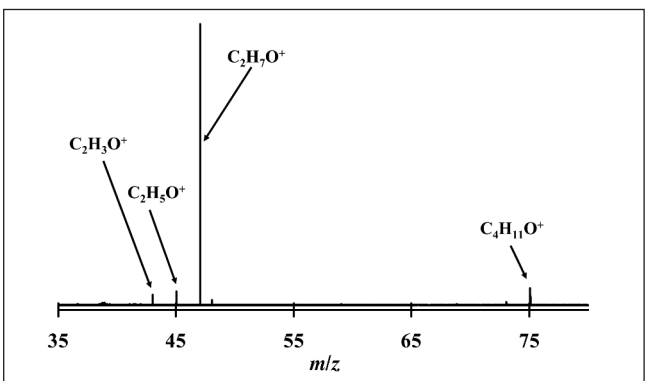

Figure 1. A representative FT-ICR mass spectrum of the (ethanol) CI reagent ions.

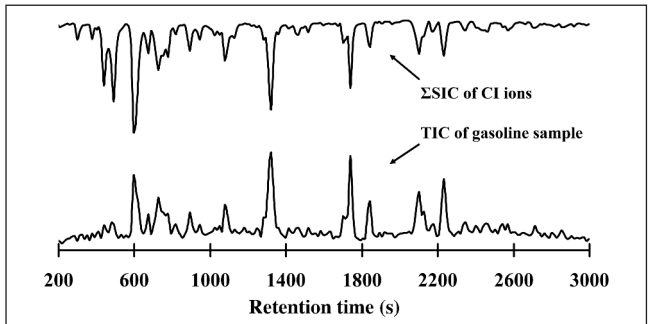

Figure 2. GC–FT-ICR CI TIC of a commercial gasoline sample.

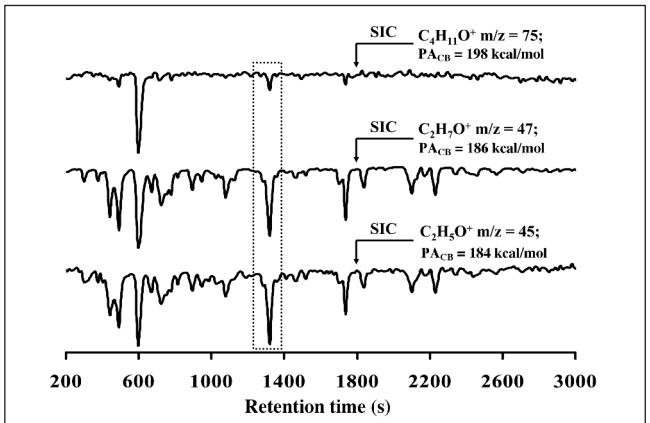

Figure 3. SICs for CI reagents from ethanol SCI reactions (in order of descending conjugate base PA values: ethyl ether, ethanol, acetaldehyde).

CI GC–FT-ICR gasoline analysis

In Figure 2, the CI GC–FT-ICR-MS TIC of a gasoline sample is shown in the bottom curve. The upper chromatogram represents the sum of all the selected ion chromatograms of the CI reagent ions [i.e., protonated ethanol (*m/z* 47), protonated acetaldehyde (*m/z* 45), and protonated ethyl ether (*m/z* 75)]. In Figure 2, the top (ESIC of reagent ion) and bottom (TIC of gasoline sample) plots are highly correlated and depletion of the reagent ions (from the top ESIC plot) occur only when there is a PT to a GC eluted compound (or compounds), as seen in the bottom trace. Figure 3, provides a more detailed analysis of the reagent ion depletions for three reagents with different PA values. In other words, Figure 3 contains the three individual SICs (normalized to 1) of the CI reagent ions. The PA values of acetaldehyde, ethanol, and ethyl ether are 183.7 kcal/mol, 185.6 kcal/mol, and 198.0 kcal/mol, respectively (47). Table I contains a summary of the selected mass measurement results for the commercial gasoline sample. Columns one through five (in Table I) contain the *m/z* values (experimental and theoretical), mass measurement errors (MME) in ppm, assigned elemental compositions, and potential parent molecules corresponding to the major components present in the analyzed sample. In this study we did not attempt to perform an exhaustive analysis of all of the observed compounds. For example, the SIC for *m/z* 85 (corresponding to $C_6H_{13}^+$) and *m/z* 99 ($C_7H_{15}^+$) show at least nine and ten GC resolved compounds corresponding to various isomers of hexene (out of possible seventeen isomers) and heptene (out of possible thirty six isomers), respectively. Conversely, the SIC for *m/z* 93 shows only a single GC peak (corresponding to elution of toluene).

Table I. Summary of Selected Mass Measurement Results from CI GC–FT-ICR-MS Analysis of an Authentic Gasoline Sample

m/z values		Elemental compositions	MME (ppm)	Potential parent molecule
Experimental	Theoretical			
43.0179	43.0178	$C_2H_3O^+$	–2.3	CI reagent
45.0335	45.0335	$C_2H_5O^+$	0.0	CI reagent
47.0491	47.0491	$C_2H_7O^+$	0.0	CI reagent
75.0804	75.0804	$C_4H_{11}O^+$	0.0	CI reagent
57.0699	57.0699	C_4H_9+	0.0	C_4H_8
71.0855	71.0855	C_5H_{11}+	0.0	C_5H_{10}
71.0854	71.0855	$C_5H_{11}^+$	1.4	C_5H_{10}
85.1009	85.1012	$C_6H_{13}^+$	3.5	C_6H_{12}
89.0958	89.0961	$C_5H_{13}O^+$	3.4	MTBE
85.1011	85.1012	$C_6H_{13}^+$	1.2	C_6H_{12}
85.1009	85.1012	$C_6H_{13}^+$	3.5	C_6H_{12}
85.1011	85.1012	$C_6H_{13}^+$	1.2	C_6H_{12}
99.1168	99.1168	$C_7H_{15}^+$	0.0	C_7H_{14}
99.1168	99.1168	$C_7H_{15}^+$	0.0	C_7H_{14}
99.1167	99.1168	$C_7H_{15}^+$	1.0	C_7H_{14}
93.0692	93.0699	$C_7H_9^+$	7.5	C_7H_8
113.1326	113.1325	$C_8H_{17}^+$	–0.9	C_8H_{16}
107.0854	107.0856	$C_8H_{11}^+$	1.9	ethylbenzene
107.0849	107.0856	$C_8H_{11}^+$	5.6	*m*-xylene
107.0854	107.0856	$C_8H_{11}^+$	1.9	*o*-,*p*-xylene
121.1008	121.1012	$C_9H_{13}^+$	3.3	C_3-Ar
121.1010	121.1012	$C_9H_{13}^+$	1.5	C_3-Ar
121.1011	121.1012	$C_9H_{13}^+$	0.8	C_3-Ar
121.1007	121.1012	$C_9H_{13}^+$	4.1	C_3-Ar
121.1011	121.1012	$C_9H_{13}^+$	0.8	C_3-Ar
135.1166	135.1168	$C_{10}H_{15}^+$	1.5	C_4-Ar
135.1168	135.1168	$C_{10}H_{15}^+$	0.0	C_4-Ar
135.1168	135.1168	$C_{10}H_{15}^+$	0.0	C_4-Ar
129.0695	129.0699	$C_{10}H_9^+$	3.1	Naphthalene

Comparing the major components listed in Table I with the MSDS sheet for commercially available gasoline samples shows that a significant deviation exists between the number of components that are regulated and the number of components present in the retail samples analyzed in our study. For example, according to the MSDS data, the "toxic chemicals" that are specifically regulated by the U.S. Environmental Protection Agency (EPA) include benzene, ethylbenzene, *n*-hexane, MTBE, toluene, 1,2,4-trimethylbenzene, and xylenes. Our chromatograms indicate the presence of over 50 GC resolved species. It should be noted that the use of reagent ions with low acid strengths in our experiments excludes the detection of low PA alkanes. Based on the MSDS data from various commercial sources, alkanes are the bulk constituents in retail gasoline samples. Most of the observed species in our GC–FT-ICR-MS ion chromatograms correspond to protonated alkenes which are presumably minor components in commercially available retail gasoline samples. Table I lists mass measurement accuracies and chemical compositions for the 25 observed major components.

Methyl *t*-butyl ether or 2-methoxy-2-methyl-propane

Figure 3 shows that at a RT of ~600 s the relative abundances of all three CI reagent SICs decrease to zero. This RT corresponds to the elution of methyl *t*-butyl ether (MTBE) from the GC column. The PA of MTBE is 201.1 kcal/mol (47). This value is higher than the conjugate base PA values of all three CI reagent ions, and, hence, MTBE molecules are protonated by all three CI reagents. Accordingly, as evidenced in SICs included in Figure 3, all CI reagent ions are depleted during the period when MTBE neutral molecules are introduced into the ICR cell.

Figure 4 shows the observed mass spectrum at RT ~600 s, assigned to MTBE. Table II includes the experimental and theoretical *m/z* values, assigned elemental compositions, MME in ppm, and the potential identities of the major components appearing in the mass spectrum at RT ~ 600 s. All mass measurement errors were within 5 ppm, and thus the chemical compositions listed in the 5th column of Table II [*viz.*, $C_4H_9^+$ (*m/z* 57), $C_5H_{13}O^+$ (*m/z* 89), $C_6H_{15}O^+$ (*m/z* 103), $C_6H_{17}O_2^+$ (*m/z* 121), $C_7H_{19}O_2^+$ (*m/z* 135), and $C_{10}H_{25}O_2^+$ (*m/z* 177)] are assigned at a high level of confidence. Both the observed mass spectral data, including the pseudo-molecular ion (viz. $[M+H]^+$ at *m/z* = 89.0958) and mass spectral pattern, and the PA data obtained from CI reagent depletions were used to make the confident assignment of MTBE to the analyte at RT ~600 s. A similar approach was used for all other major components present in the gasoline sample.

Isomers of C_7H_8

In Figure 3, a box was placed around the reagent depletions corresponding to RT ~1320 s. From the accurate mass measurement, the chemical composition of the analyte(s) eluting at RT

~1320 s can be confidently assigned as C_7H_8. However, in the following section we demonstrate that our thermochemical data provides further clues about the identities of the presumed C_7H_8 species. Specifically, ion-molecule reactions show that the GC peak at RT ~1320 s is composed of more than one structural isomer of this chemical formula.

Toluene is one of the most prevalent components in retail gasoline products. As a result, the analyte at RT ~1320 s was initially assigned to toluene alone. Upon closer examination, additional information was obtained. In Figure 3, depletions of all three reagent ions at the GC RT of ~1320 s, demonstrate that the analyte eluting at this RT has a higher PA value than all three CI reagents. However, the PA value of toluene from the literature is 187.4 kcal/mol (47). Hence, proton transfer from protonated ethyl ether to toluene is unlikely. These results suggest that the PA value of an analyte contained in this peak (co-eluting with toluene) is higher than 198.0 kcal/mol. Considering the available thermochemical data in the literature, 1,3,5-cycloheptatriene (CHT), with a PA of 833 ± 4 kJ/mol (e.g., ~200 kcal/mol) (48), can be considered as a plausible co-eluting C_7H_8 isomer at ~1320 s. In the next section, we discuss the investigation of authentic toluene and CHT samples utilized to rule out this possibility.

Analysis of standard toluene and 1,3,5-cycloheptatriene samples

Both mixtures and individual samples of authentic toluene and CHT were analyzed to affirm or reject the hypothesis that a co-eluting analyte at RT ~1320 s was CHT. Specifically, electron impact GC–FT-ICR experiments were performed to confirm the RT of toluene and CHT. Under the identical GC conditions used for the analysis of the gasoline sample, toluene and CHT did not co-elute. Specifically, the RT of toluene was indeed confirmed as ~1320 s, but the RT of CHT was ~1460 s. Therefore, CHT was rejected as a co-eluting C_7H_8 isomer of toluene.

Although CHT was eliminated based on its RT, CI experiments of standard toluene and CHT were performed to confirm that the peak at ~ 1320 s was a composite of toluene and at least one more component with a higher proton affinity. The CI reagents used for the gasoline sample (viz. protonated ethanol, protonated acetaldehyde, and protonated ethyl ether) were used to analyze the standard C_7H_8 compounds. Representative results from these experiments are shown in Figures 5 and 6 (under different GC experimental conditions). However, we performed multiple experiments under varied experimental conditions to confirm our findings. To ensure reproducibility, CI GC–FT-ICR chromatograms were obtained by injecting six portions of headspace at 2 min intervals in a 25 min long experiment. For the sake of clarity, only one set of analyte/reagent peaks is displayed for toluene and CHT.

Figure 5 contains SICs for protonated toluene, ethanol, acetaldehyde, and ethyl ether. Figure 5 shows that toluene depletes protonated acetaldehyde and protonated ethanol, but not protonated ethyl ether. These results are in agreement with the experimental PA of toluene [viz., 187.4 kcal/mol (47)]. Figure 6 contains SICs for protonated CHT and the same CI reagents shown in Figure 5. It is shown that although toluene does not deplete protonated ethyl ether, CHT (with a PA of 200 kcal/mol) does deplete this reagent. In the commercial gasoline sample, protonated ethyl ether was depleted at RT ~1320 s (see Figure 3). Thus, the analyses of standard toluene and CHT confirm that the peak at RT ~1320 s in the commercial gasoline sample contains both toluene and one or more co-eluting analyte(s) with a higher PA than that of ethyl ether (viz. 198.0 kcal/mol). Based on the RT, CHT can be ruled out as the other isomer. Possible structures for $C_7H_9^+$ species were discussed in an earlier publication (44), and it is not convenient to determine the RT for all potential species [e.g., 2,5-norbornadiene, 6-methylfulvene, 3-methylene1, 4 Cyclohexadiene, spiro (2,4) hepta-4, 6-diene, bicyclo (3.2.0) hepta-2, 6-diene, 1, 6-heptadiyne, cyclopropane, 1-ethynyl-1-ethenyl, etc.]. However, we are currently using *ab initio* calcula-

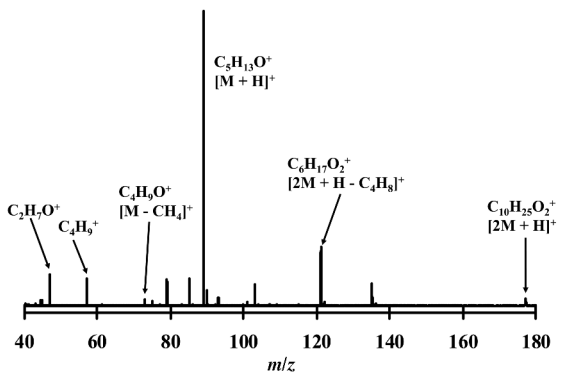

Figure 4. The CI FT-ICR mass spectrum of methyl tertiary-butyl ether (M).

Table II. Observed CI GC–FT-ICR MS Ions for MTBE

m/z Values		Elemental Compostions	MME (ppm)	Potential Identity
Experimental	Theoretical			
47.0491	47.0491	$C_2H_7O^+$	0.0	CI reagent
57.0697	57.0699	$C_4H_9^+$	3.5	$[M–CH_4O]^+$
73.0646	73.0648	$C_4H_9O^+$	2.7	$[M–CH_4]^+$
89.0958	89.0961	$C_5H_{13}O^+$	3.4	$[M+H]^+$
90.0994	90.0995	$^{13}CC_4H_{13}O^+$	1.1	$[M+H]^+$
103.1115	103.1117	$C_6H_{15}O^+$	1.9	$[2M+H–C_4H_{10}O]^+$
121.1219	121.1223	$C_6H_{17}O_2^+$	3.3	$[2M+H–C_4H_8]^+$
135.1374	135.1380	$C_7H_{19}O_2^+$	4.4	$[M+H+C_2H_6O]^+$
177.1851	177.1849	$C_{10}H_{25}O_2^+$	–1.1	$[2M+H]^+$

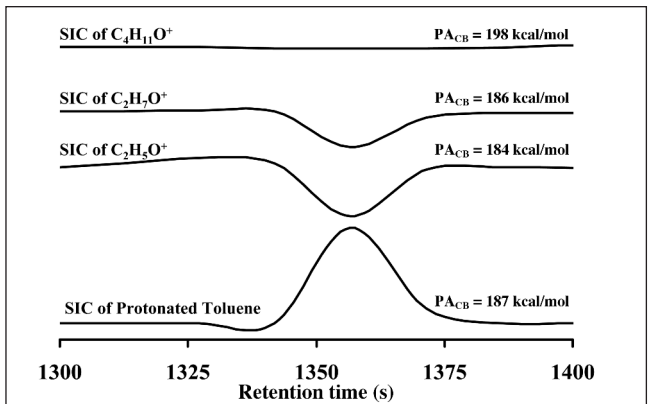

Figure 5. SICs from bottom to top for standard toluene (analyte), protonated acetaldehyde, protonated ethanol, and protonated ether.

tions to search for potential C7H8 isomers that have high PA values that could deplete the protonated ethyl ether reagent ions.

In the "GC–FT-ICR-CI-MS of Standard C_8H_{10} Samples" Section, results of additional CI MS experiments with authentic toluene and different reagents are discussed. It is shown that there is no proton transfer reaction between toluene and acetone. Hence, it is further affirmed that the analyzed "real world" gasoline sample contains other isomer(s) of C_7H_8 that co-elute with toluene under our GC conditions.

Isomers of C_8H_{10}/C_2-Ar

The top three plots in Figure 7 correspond to the SICs of the CI reagent ions (similar to Figure 3). However, the bottom plot shows the SIC for protonated C_2-Ar (*m/z* = 107 amu). The 3 peaks at RTs ~1700 s, 1740 s, 1840 s (labeled A, B, and C, respectively) show that there are at least 3 components of chemical composition C_8H_{10}, based on accurate mass measurement (see Table I). Here, C_2-Ar or C_2-aromatic is used to denote molecules (C_8H_{10}) that contain one aromatic ring with two attached carbon groups (C_2) at various possible positions and/or configurations. This confident chemical formula information and the PA bracketing discussed below were used to assign the peaks A, B, and C to ethylbenzene, *m*-xylene, and *o*-/*p*-xylene, respectively. As expected, GC separation pattern or co-elution order of the C_8H_{10}/C_2-Ar set of isomers depends on the type of stationary phase used.

Figure 7 shows that at RT ~1700 s, the intensities of the SICs of protonated acetaldehyde and protonated ethanol (with PAs of the conjugate bases being 183.7 kcal/mol and 185.6 kcal/mol, respectively) decrease. Conversely, at the same RT ~1700 s, the other SIC corresponding to protonated ether (with a PA of the conjugate base of 198.0 kcal/mol) remains undepleted. Therefore, data in Figure 7 demonstrates that the PA of the GC eluted analyte at 1700 s is higher than 185.6 kcal/mol but lower than 198 kcal/mol. The PA value of ethylbenzene is 188.3 kcal/mol (47). Hence, the observed GC peak at 1700 s is consistent with ethylbenzene.

At a RT of ~1740 s, the intensities of the SICs of protonated acetaldehyde and protonated ethanol are diminished, while intensities of the other SIC (protonated ether) is slightly depleted. Therefore, the PA value of this analyte is higher than 185.6 kcal/mol, and much closer to 198 kcal/mol than ethylbenzene. The PA value of *m*-xylene is 194.1 kcal/mol (47). Thus, again, by PA bracketing, the GC peak at 1740 s can be assigned as to *m*-xylene based on the aforesaid observation. It should be noted that the proton transfer reaction efficiency for this system is less than unity (38).

The mass spectral pattern of the GC peak at 1840 s is quite similar to the mass spectral pattern for GC effluent of 1700 s. In Figure 7, the changes in the SICs at the GC RT of 1840 s demonstrate that the PA value of this GC effluent was higher than 185 kcal/mol but was not close to 198 kcal/mol (i.e., no depletion is observed in the SIC of protonated ether). The PA values of *o*-xylene and *p*-xylene (e.g., 190.2 kcal/mol and 189.9 kcal/mol) both agree with these experimental results. This GC peak could be one of these two C_2-Ar isomers (e.g., just *o*-xylene or *p*-xylene) or their mixture. It is worth noting that MS–MS experiments on GC eluting species could potentially provide complementary and useful information on analytes that have different fragmentation patterns. However, in FT-ICR-MS, a prior knowledge about the molecular size (i.e., ICR frequency) is required to perform controlled collision activated dissociation experiments. However, prior knowledge about the molecular weight is not required to perform ion-molecule reactions. Hence and alternatively, a series of reagent ions with smaller PA differences could be used to further improve the resolution in this type of analysis. Such an improvement was implemented, and the results are discussed in the following section.

GC–FT-ICR-CI-MS of standard C_8H_{10} samples

A mixture of standard samples (e.g., 3-pentanone, toluene, ethylbenzene, and each of the three xylene isomers) was analyzed using CI GC–FT-ICR MS in order to both validate our method and further confirm the results discussed for the authentic gasoline sample (i.e., see "Isomers of C_7H_8" and "Isomers of C_8H_{10}/C_2-Ar") These standard experiments were performed under identical experimental conditions (e.g., GC temperature programming, GC head pressure, etc.) as the CI MS analyses of gasoline samples (as described earlier). In these experiments, a 0.2 µL liquid from each of the 6 chemicals was transferred into an N_2 filled 40 mL EPA vial. A 5 µL portion of head space was withdrawn from this 40 mL vial and then injected onto the GC for GC–MS analysis.

The CI reagents used for these standard analyses were

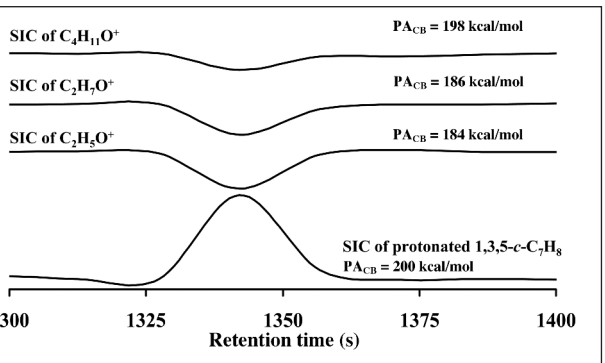

Figure 6. Selected ion chromatograms (SICs) from bottom to top for standard 1,3,5-cycloheptatriene (analyte), protonated acetaldehyde, protonated ethanol, and protonated ether.

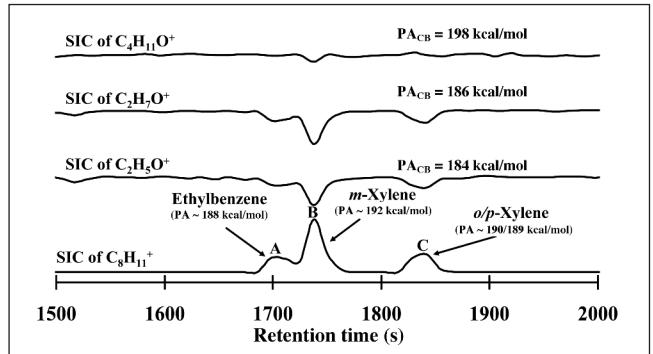

Figure 7. SICs for *m/z* 107 (bottom plot, the SIC of C2-Aromatics) and three CI reagent ions 75, 47, 45 [in order of descending conjugate base PA values: ethyl ether (PA = 198.0 kcal/mol), ethanol (PA = 185.6 kcal/mol), and acetaldehyde (PA= 183.7.0 kcal/mol)]. The labels A (ethylbenzene), B (m-xylene), and C (a mixture of *o*-xylene + *p*-xylene) in bottom plot correspond to various isomers of C_8H_{10}.

methanol, ethanol, isopropanol, and acetone. The PA values of these chemicals are 180.3 kcal/mol, 185.6 kcal/mol, 189.5 kcal/mol, and 194.0 kcal/mol, respectively (47). It should be noted that at high concentrations of methanol, an ion at *m/z* 47 can be produced (viz., protonated dimethyl ether $–CH_3OH^+CH_3$ with PA of ~ 189 kcal/mol) (49). In preparing the reagent sample mixture, low concentrations of methanol were used in the sample reservoir to reduce/eliminate the formation of the protonated dimethyl ether.

In Figure 8, the top four chromatograms correspond to the protonated CI reagents: acetone, isopropanol, ethanol, and methanol. The peaks in the bottom chromatogram correspond to the elution of 3-pentanone, toluene, ethylbenzene, and *m*-xylene (from lowest to highest RT), with PA values of 200.0 kcal/mol, 187.4 kcal/mol, 188.3 kcal/mol, and 194.0 kcal/mol, respectively (47). The peak labeled as *o/p*-xylene contains a mixture of co-eluting *o*-xylene (PA = 190.2 kcal/mol) and *p*-xylene (PA = 189.9 kcal/mol) isomers (22).

The PA of 3-pentanone is higher than the conjugate bases of all the CI reagent ions. As expected, intensities of the reagent SICs are depleted during the elution of 3-pentanone.

The PA of toluene is ~ 7 kcal/mol lower than acetone but higher than the other three CI reagents. Accordingly, Figure 8 shows that proton transfers occur from protonated methanol, ethanol, and isopropanol to neutral toluene. However, protonated acetone is not depleted during the elution of toluene. Hence, these results provide further support for the arguments discussed in the earlier sections (viz. "CI GC–FT-ICR gasoline analysis" and "Analysis of standard toluene and 1,3,5-cycloheptatriene samples") addressing the PA measurements of the peak at RT ~ 1320 s in the commercial gasoline sample (i.e., the impurity of C_7H_8 species and isomer differentiation).

Figure 8 also shows that the GC peak for ethylbenzene has corresponding depletions in all the CI reagents except acetone. Although the PA of ethylbenzene is 188.3 kcal/mol, it does deplete protonated isopropanol (PACB of 189.5 kcal/mol). It is important to note that proton transfer at a reduced reaction rate will occur between a reagent ion and a neutral analyte even when the analyte has a lower proton affinity. For example, in the absence of proton transfer barriers, for a PA difference of ~ 5 kcal/mol the reaction efficiency can be reduced to ~ 8×10^{-4} at room temperature (50).

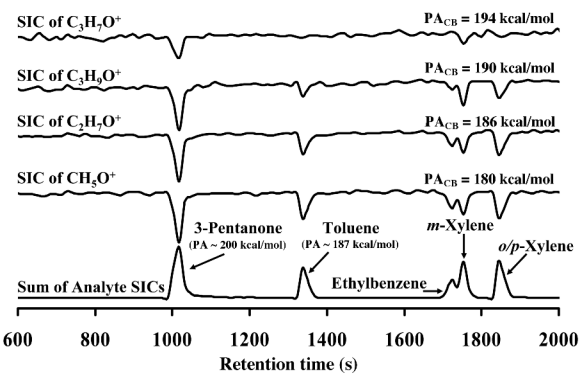

Figure 8. SICs for 6 authentic chemical samples (bottom plot) and CI reagent ions [in the order of descending conjugate bases PA values: acetone (PA = 194.0 kcal/mol), isopropanol (PA = 189.5 kcal/mol), ethanol (PA = 185.6 kcal/mol), and methanol (PA = 180.3 kcal/mol)] are shown. The peaks from the standard mixture are labeled 3-pentanone, toluene, ethylbenzene, *m*-xylene, and *o,p*-xylene in the bottom plot.

The fifth major GC peak in Figure 8 (RT >1800 s) is a mixture of *o*-, and *p*-xylenes. It has been noted that these two isomers are difficult to separate by one dimensional GC (51); using our GC column and changing the GC temperature programming and/or head pressure did not allow complete separation of these two species. The co-elution of *o*- and *p*-xylene under our experimental conditions limits the bracketing of their PA values.

Conclusions

GC–FT-ICR-MS is a powerful analytical technique and offers unparalleled mass measurement accuracy for analyzing complex mixtures. Molecular fingerprinting and unknown identification at a high level of confidence are possible by combining unique advantages of FT-ICR-MS (e.g., ion-molecule reaction kinetics). Accurate mass measurement of unknown analytes at low concentrations is feasible with CI GC–FT-ICR. Moreover, this approach provides additional dimensions of analysis, such as multiple PA measurements, that yield higher analytical resolution for accurate "sample printing". Combination of the high mass resolving power and accurate determination of thermochemical properties by CI GC–FT-ICR-MS provides unique opportunities for characterization of complex samples. Simultaneous determination of thermochemical properties using both CI GC–FT-ICR-MS experimental approaches and ab initio theoretical calculations should permit identification of unknown species that are not present in the current commercial libraries.

Acknowledgments

Financial support from the U.S. Department of Defense (DOD Contract # CDMRP-OC060322) and U. S. Geological Survey USGS (Contract # 2006ME94G) is greatly acknowledged. The authors wish to thank Dr. Jan E. Szulejko for helpful discussions. The views and conclusions contained in this document are those of the authors and should not be interpreted as necessarily representing the official policies, either expressed or implied, of the U.S. Government.

References

1. L. Singer. Summary of the improvements in analytical methods of the petroleum industry. *Petroleum (London)* **4:** 977 (1909).
2. H. Hoover and H. Washburn. A preliminary report on the application of the mass spectrometer to problems in the petroleum industry. *Trans. Am. Inst. Mining Metall. Eng.* **142:** 100–106 (1941).
3. N.D. Coggeshall and W. Hubis. The combination of methods in the analysis of complex hydrocarbon systems. *Am. Soc. Testing Materials Spec. Tech. Publ.* **269:** 195–214 (1960).
4. A.G. Marshall and R.P. Rodgers. Petroleomics: The next grand challenge for chemical analysis. *Acc. Chem. Res.* **37:** 53–59 (2004).
5. C.A. Hughey, R.P. Rodgers, A.G. Marshall, C.C. Walters, K. Qian, and P. Mankiewicz. Acidic and neutral polar NSO compounds in smackover oils of different thermal maturity revealed by electrospray high field fourier transform ion cyclotron resonance mass spectrometry. *Org. Geochem.* **35:** 863–80 (2004).

6. Z. Wang and M. Fingas. Differentiation of the source of spilled oil and monitoring of the oil weathering process using gas chromatography–mass spectrometry. *J. Chromatogr. A* **712:** 321–43 (1995).
7. R.P. Rodgers, E.N. Blumer, M.A. Freitas, and A.G. Marshall. Compositional analysis for identification of arson accelerants by electron ionization fourier transform ion cyclotron resonance high-resolution mass spectrometry. *J. Forensic Sci.* **46:** 268–79 (2001).
8. J.E. Szulejko and T. Solouki. Potential analytical applications of interfacing a GC to an FT-ICR MS: Fingerprinting complex sample matrixes. *Anal. Chem.* **74:** 3434–42 (2002).
9. P.M.L. Sandercock and E.D. Pasquier. Chemical fingerprinting of unevaporated automotive gasoline samples. *Forensic Sci. Int.* **134:** 1–10 (2003).
10. S.A. Stout. Applications of petroleum fingerprinting in known and suspected pipeline releases—Two case studies. *Appl. Geochem.* **18:** 915–26 (2003).
11. Z. Wang and M.F. Fingas. Development of oil hydrocarbon fingerprinting and identification techniques. *Mar. Pollut. Bull.* **47:** 423–52 (2003).
12. K. Euliss, C.-H. Ho, A.P. Schwab, S. Rock, and M.K. Banks. Greenhouse and field assessment of phytoremediation for petroleum contaminants in a riparian zone. *Bioresour. Technol.* **99:** 1961–71 (2008).
13. D.T. Rogers, M.M. Kaufman, and K.S. Murray. Improving environmental risk management through historical impact assessments. *J. Air Waste Manag. Assoc.* **56:** 816–23 (2006).
14. J. Beens, H.T. Feuerhelm, J.-C. Froehling, J. Watt, and G. Schaatsbergen. A comparison of ten different methods for the analysis of saturates, olefins, benzene, total aromatics, and oxygenates in finished gasolines. *J. Chromatogr. Sci.* **41:** 564–69 (2003).
15. R.P. Rodgers, T.M. Schaub, and A.G. Marshall. Petroleomics: MS returns to its roots. *Anal. Chem.* **77:** 20–27A (2005).
16. Z. Wang, S.A. Stout, and M. Fingas. Forensic fingerprinting of biomarkers for oil spill characterization and source identification. *Environ. Forensics* **7:** 105–46 (2006).
17. D.P. Frueh, T. Ito, J.-S. Li, G. Wagner, S.J. Glaser, and N. Khaneja. Sensitivity enhancement in NMR of macromolecules by application of optimal control theory. *J. Biomol. NMR* **32:** 23–30 (2005).
18. A.E. Kelly, H.D. Ou, R. Withers, and V. Dotsch. Low-conductivity buffers for high-sensitivity NMR measurements. *J. Am. Chem. Soc.* **124:** 12013–12019 (2002).
19. D. Nedelkov, A. Rasooly, and R.W. Nelson. Multitoxin biosensor-mass spectrometry analysis: A new approach for rapid, real-time, sensitive analysis of staphylococcal toxins in food. *Int. J. Food Microb.* **60:** 1–13 (2000).
20. M.R. Emmett, F.M. White, C.L. Hendrickson, S.D.-H. Shi, and A.G. Marshall. Application of micro-electrospray liquid chromatography techniques to FT-ICR MS to enable high-sensitivity biological analysis. *J. Am. Soc. Mass Spectrom.* **9:** 333–40 (1998).
21. T. Solouki, J.E. Szulejko, J.B. Bennett, and L.B. Graham. A preconcentrator coupled to a GC/FTMS: Advantages of self-chemical ionization, mass measurement accuracy, and high mass resolving power for GC applications. *J. Am. Soc. Mass Spec.* **15:** 1191–1200 (2004).
22. http://nist.gov, Chemistry Online Webbook (2005).
23. N. Ragunathan, K.A. Krock, C. Klawun, T.A. Sasaki, and C.L. Wilkins. Gas chromatography with spectroscopic detectors. *J. Chromatogr. A* **856:** 349–97 (1999).
24. S.D. Richardson. The role of GC–MS and LC–MS in the discovery of drinking water disinfection by-products. *J. Environ. Monit.* **4:** 1–9 (2002).
25. X. Zhang, R.A. Minear, Y. Guo, C.J. Hwang, S.E. Barrett, K. Ikeda, Y. Shimizu, and S. Matsui. An electrospray ionization-tandem mass spectrometry method for identifying chlorinated drinking water disinfection byproducts. *Water Res.* **38:** 3920–30 (2004).
26. A. Fievre, T. Solouki, M. Alan, and W.T. Cooper. High-resolution Fourier transform ion cyclotron resonance mass spectrometry of humic and fulvic acids by laser desorption/ionization and electrospray ionization. *Energy Fuels* **11:** 545–60 (1997).
27. T.J. Francl, M.G. Sherman, R.L. Hunter, M.J. Locke, W.D. Bowers, J. Robert, and T. McIver. Experimental Determination of the Effects of Space Charge on Ion Cyclotron Resonance Frequencies. *Int. J. Mass Spectrom. Ion Proc.* **54:** 189–99 (1983).
28. A.G. Marshall and P.B. Grosshans. Fourier transform ion cyclotron resonance mass spectrometry: The teenage years. *Anal. Chem.* **63:** 215A–29A (1991).
29. D.A. Peake and M.L. Gross. Iron (I) chemical ionization and tandem mass spectrometry for locating double bonds. *Anal. Chem.* **57:** 115–20 (1985).
30. D.A. Peake, S.-K. Huang, and M.L. Gross. Iron(I) chemical ionization for analysis of alkene and alkyne mixtures by tandem sector mass spectrometry or gas chromatography/Fourier transform mass spectrometry. *Anal. Chem.* **59:** 1557–63 (1987).
31. S.G. Roussis and J.W. Fedora. Determination of alkenes in hydrocarbon matrices by acetone chemical ionization mass spectrometry. *Anal. Chem.* **69:** 1550–56 (1997).
32. R. Chal and A.G. Harrison. Location of double bonds by chemical ionization mass spectrometry. *Anal. Chem.* **53:** 34–37 (1981).
33. D.A. Peake, M.L. Gross, and D.P. Ridge. Mechanism of the reaction of gas-phase iron ions with neutral olefins. *J. Am. Chem. Soc.* **106:** 4307–16 (1984).
34. M.S.B. Munson and F.H. Field. Chemical ionization mass spectrometry. I. General introduction. *J. Am. Chem. Soc.* **88:** 2621–30 (1966).
35. M.S.B. Munson and F.H. Field. Chemical ionization mass spectrometry. II. Esters. *J. Am. Chem. Soc.* **88:** 4337–45 (1966).
36. D.E. Games. Soft ionization mass spectral methods for lipid analysis. *Chem. Phys. Lipids* **21:** 389–402 (1978).
37. B. Munson. Development of chemical ionization mass spectrometry. *Int. J. Mass Spectrom.* **200:** 243–51 (2000).
38. J.E. Szulejko, Z. Luo, and T. Solouki. Simultaneous determination of analyte concentrations, gas-phase basicities, and proton transfer kinetics using gas chromatography/Fourier transform ion cyclotron resonance mass spectrometry. *Int. J. Mass Spectrom.* **257:** 16–26 (2006).
39. C.B. Jacoby, D.L. Rempel, and M.L. Gross. A cold trap/pulsed valve GC/FTMS interface: Ultra-trace analysis. Presented at the 38th ASMS Conference on Mass Spectrometry and Allied Topics. Tucson, AZ, 840–41 (1990).
40. C. Heffner, I. Silwal, J.M. Peckenham, and T. Solouki. Emerging technologies for identification of disinfection by-products: GC/FT-ICR MS characterization of solvent artifacts. *Environ. Sci. Technol.* **41:** 5419–25 (2007).
41. P.C. Burgers, J.L. Holmes, J.E. Szulejko, A.A. Mommers, and J.K. Terlouw. The gas phase ion chemistry of the acetyl cation and isomeric $[C_2H_3O]^+$ ions. *Org. Mass Spectrom.* **18:** 254–62 (1983).
42. M.N. Danchevskaya and S.N. Torbin. A study of the mechanism of dissociative ionization of the ethanol molecule by electron impact. *Adv. Mass Spectrom.* **7B:** 1314–17 (1978).
43. V.G. Anicich. An index of the literature for bimolecular gas phase cation-molecule reaction kinetics. JPL-Publication-03-19 (2003).
44. T. Solouki and J.E. Szulejko. Bimolecular and unimolecular contributions to the disparate self-chemical ionizations of a-pinene and camphene isomers. *J. Am. Soc. Mass Spectrom.* **18:** 2026–39 (2007).
45. J.E. Szulejko and T.B. McMahon. Progress toward an absolute gas-phase proton affinity scale. *J. Am. Chem. Soc.* **115:** 7839–48 (1993).
46. J.E. Szulejko, J. Hrusak, and T.B. McMahon. Combined experimental and theoretical study of the protonation of polyfluorobenzenes $[C_6H_6$-nFn] (n = 0–6). *J. Mass Spectrom.* **32:** 494–506 (1997).
47. E.P. Hunter and S.G. Lias. Evaluated gas phase basicities and proton affinities of molecules: An update. *J. Phys. Chem. Ref. Data* **27:** 413–656 (1998).
48. J.-Y. Salpin, M. Mormann, J. Tortajada, M.-T. Nguyen, and D. Kuck. The gas-phase basicity and proton affinity of 1,3,5-cycloheptatriene-energetics, structure and interconversion of dihydrotropylium ions. *Eur. J. Mass Spectrom.* **9:** 361–76 (2003).
49. J.C. Kleingeld and N.M.M. Nibbering. A Fourier-transform ion cyclotron resonance study of the mechanism of formation of protonated dimethyl ether from methanol by use of naturally occurring 18O. *Org. Mass Spectrom.* **17:** 136–39 (1982).
50. G. Bouchoux, J.Y. Salpin, and D. Leblanc. A relationship between the kinetics and thermochemistry of proton transfer reactions in the gas phase. *Int. J. Mass Spectrom. Ion Proc.* **153:** 37–48 (1996).
51. B. Sulikowski. Chromatographic separation of xylene isomers. *Pol. Czas. Tech.* **80:** 33–36 (1976).

Manuscript received July 19, 2008;
revision received October 14, 2008.